

Supporting information for

Bioinspired Multifunctional Melanin-Based Nanoliposome for Photoacoustic/Magnetic Resonance Imaging-Guided Efficient Photothermal Ablation of Cancer

Liang Zhang^{1*}, Danli Sheng^{2*}, Dong Wang^{1✉}, Yuanzhi Yao³, Ke Yang¹, Zhigang Wang², Liming
Deng², Yu Chen^{4✉}

¹Department of Ultrasound, The First Affiliated Hospital of Chongqing Medical University, Chongqing 400016, P. R. China;

²Institute of Ultrasound Imaging, The Second Affiliated Hospital of Chongqing Medical University, Chongqing, 400010, P. R. China;

³Department of Ultrasound, Chongqing Cancer Hospital, Chongqing Cancer Institute, Chongqing Cancer Center, Chongqing 400030, P. R. China;

⁴State Key Laboratory of High Performance Ceramics and Superfine Microstructures, Shanghai Institute of Ceramics, Chinese Academy of Sciences, Shanghai, 200050, P. R. China.

* These two authors contributed equally to this work.

✉ Corresponding author: D. Wang (wang57554@163.com); Y. Chen (chenyu@mail.sic.ac.cn)

Supplementary Figures

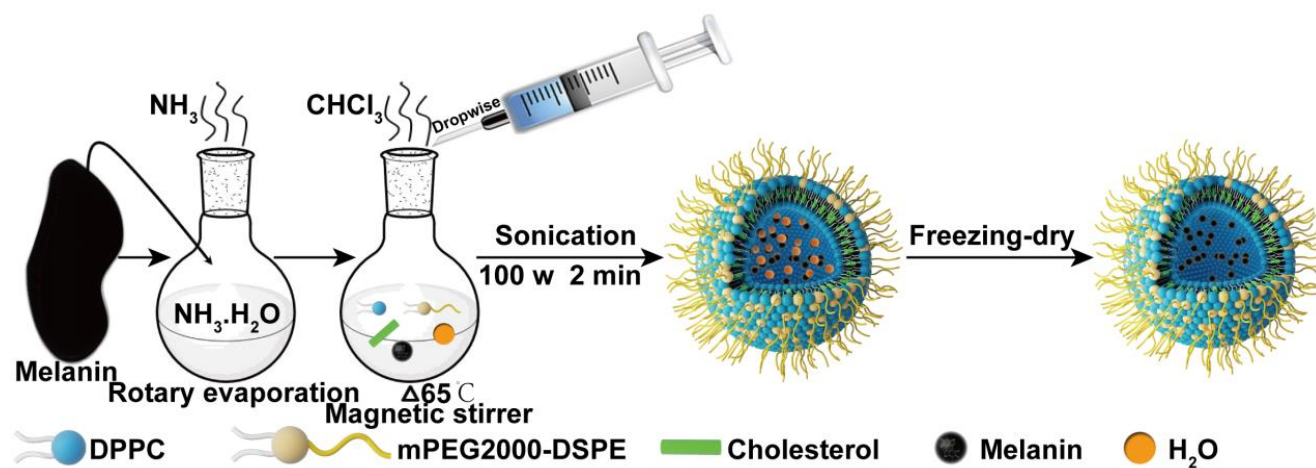


Figure S1. Schematic illustration of detailed synthetic procedure for multifunctional Lip-Mel.

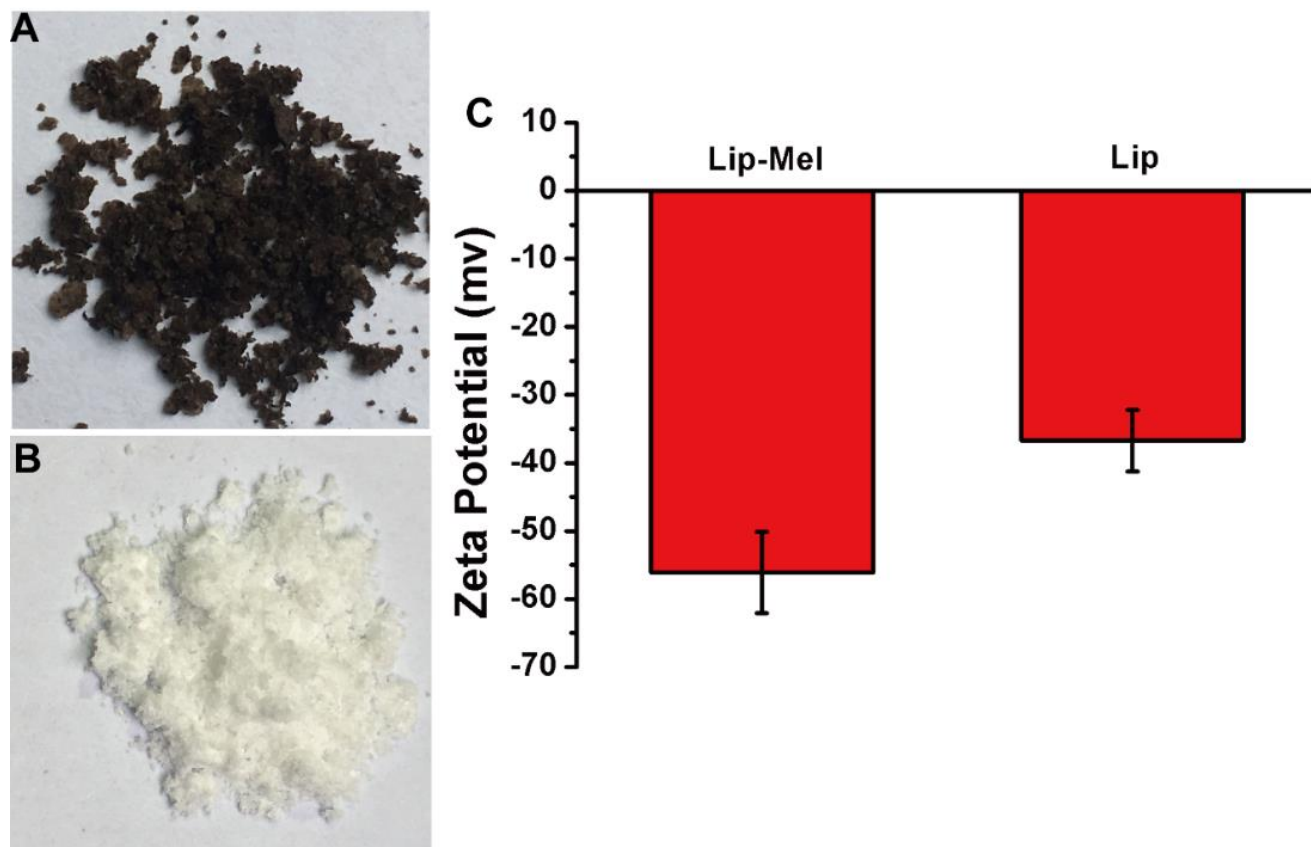


Figure S2. Photographs of lyophilized powder of (A) Lip-Mel and (B) Lip; (C) Zeta potential of Lip-Mel and Lip.

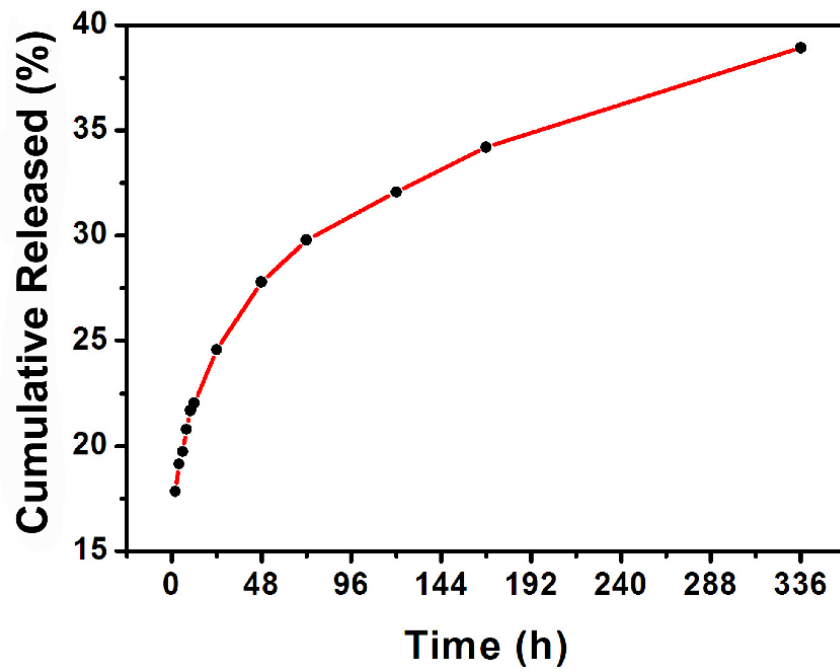


Figure S3. *In vitro* release profile of melanin from Lip-Mel nanocomposite in PBS.

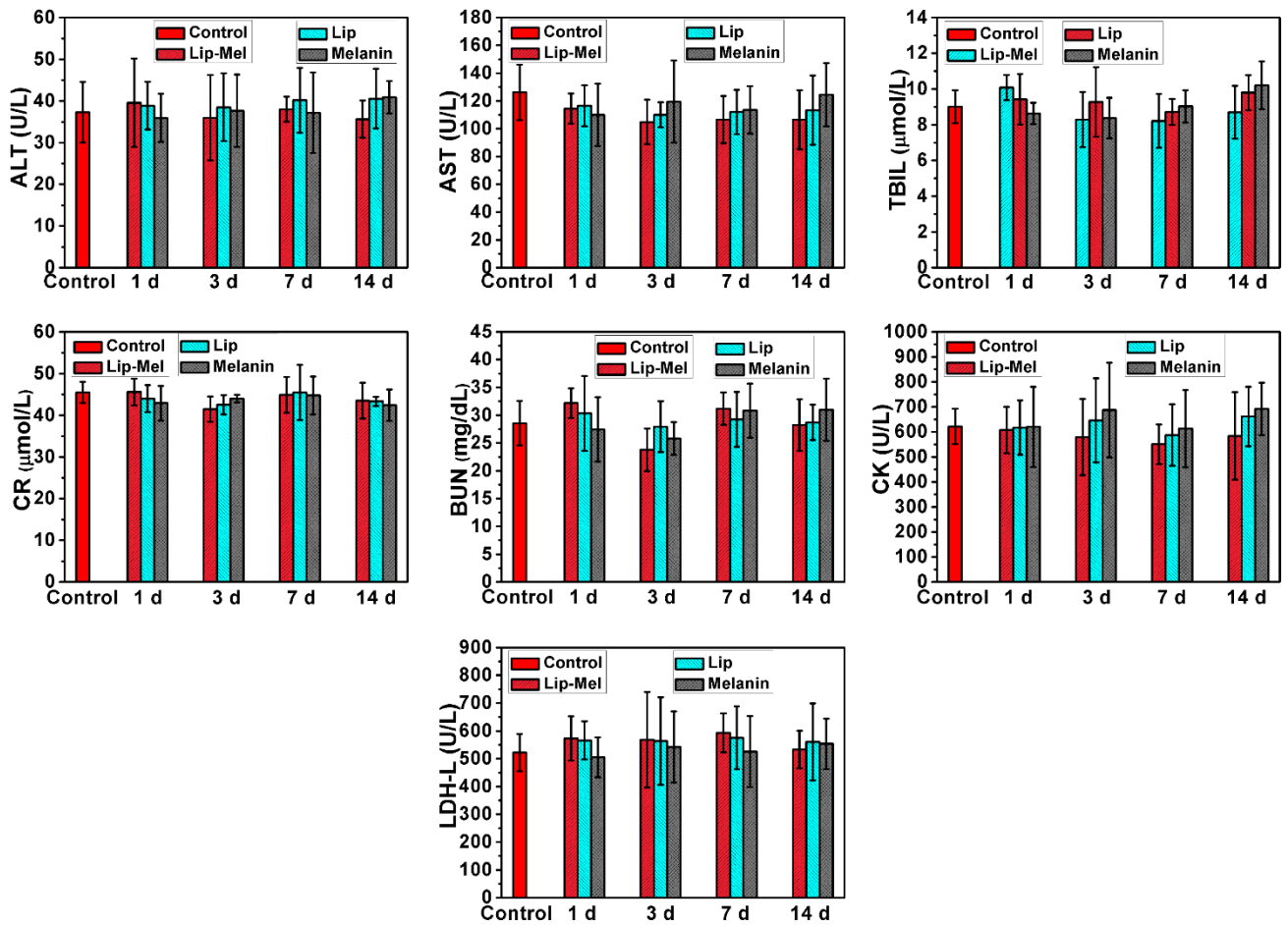


Figure S4. Serum biochemical indexes analysis of BALB/c mice from the control group and the experimental groups 1, 3, 7 and 14 days post intravenous injection of Lip-Mel, Lip and melanin.

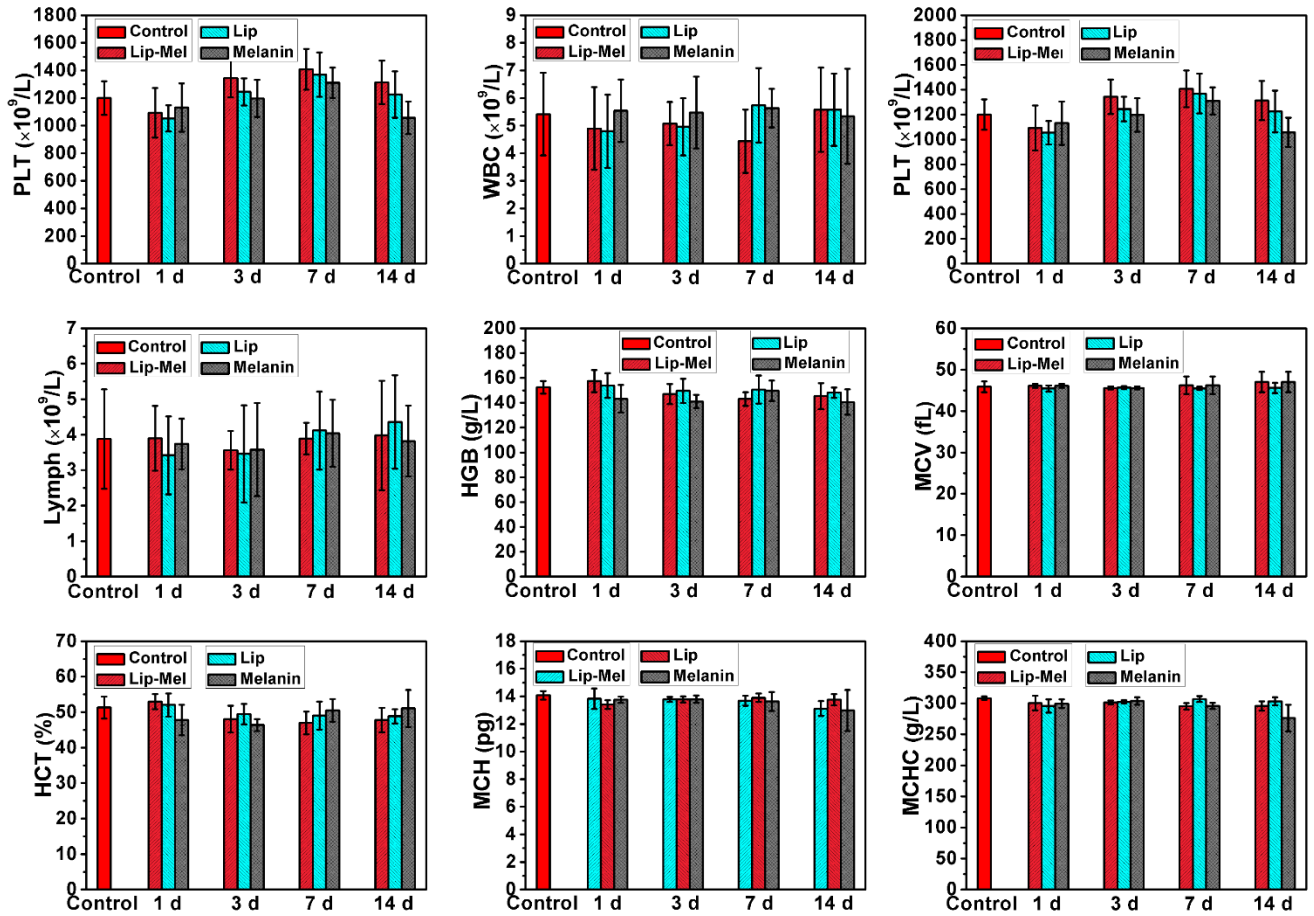


Figure S5. Routine blood examination of BALB/c mice from the control group and the experimental groups 1, 3, 7 and 14 days post intravenous injection of Lip-Mel, Lip and melanin.

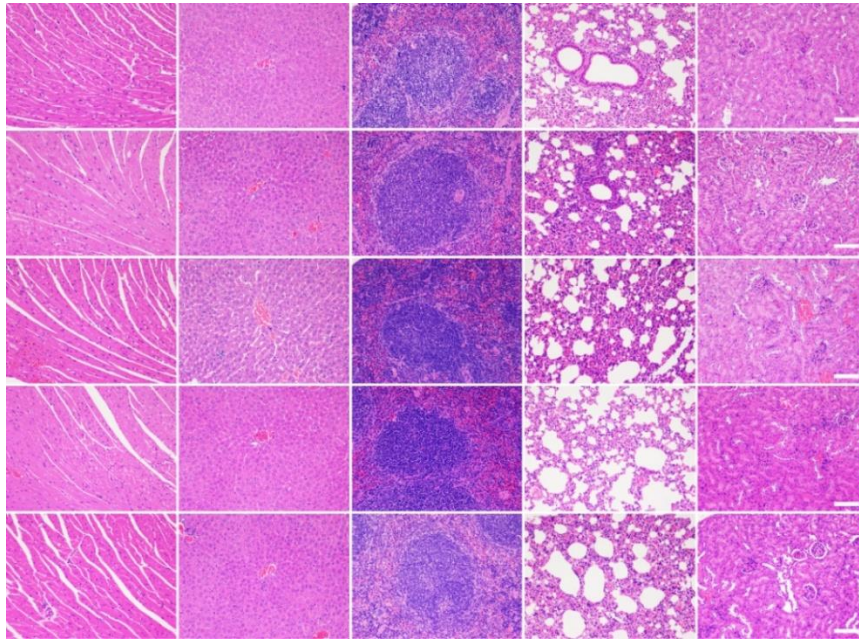


Figure S6. H&E staining of major organs from the control group. All the scale bars are 100 μm .

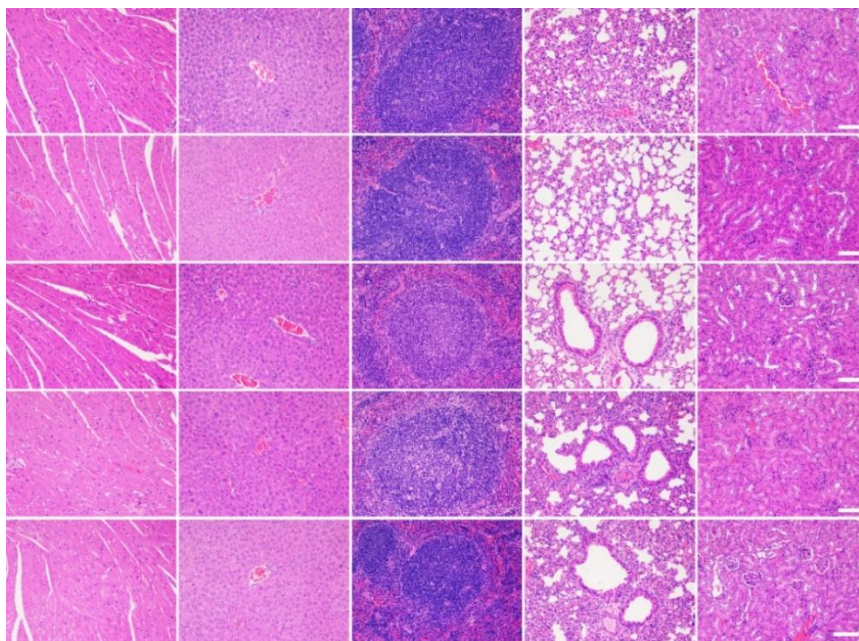


Figure S7. H&E staining of major organs from the experimental group 1 day post intravenous injection of Lip-Mel. All the scale bars are 100 μm .

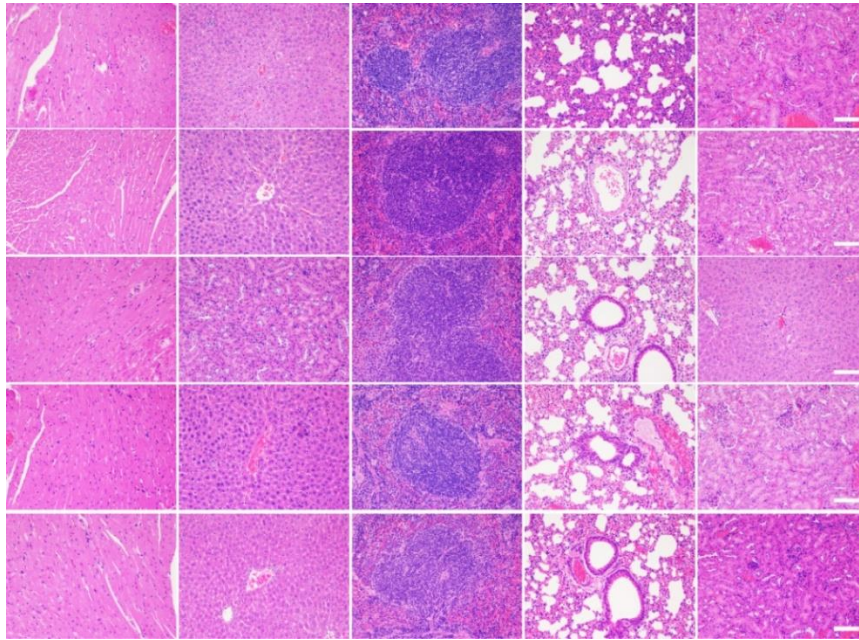


Figure S8. H&E staining of major organs from the experimental group 1 day post intravenous injection of Lip. All the scale bars are 100 μ m.

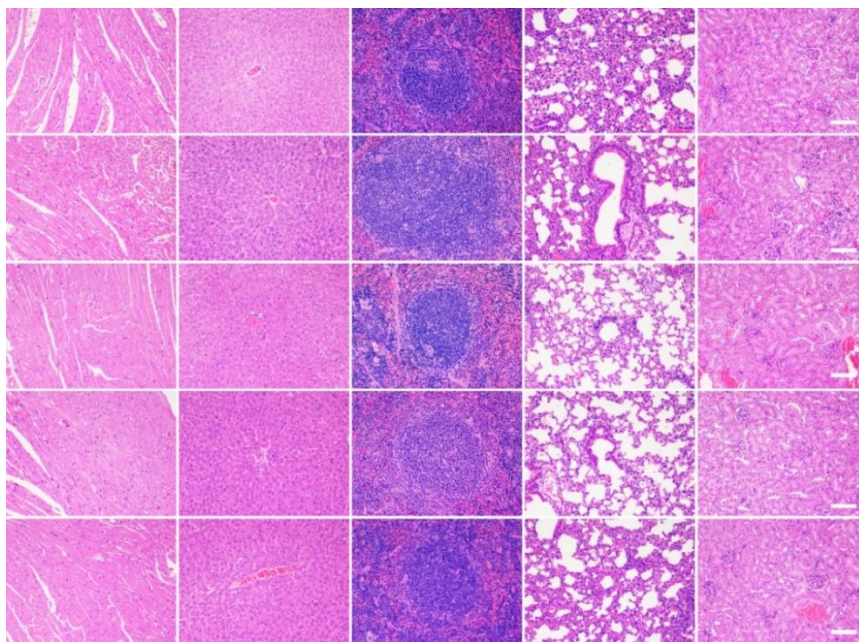


Figure S9. H&E staining of major organs from the experimental group 1 day post intravenous injection of Mel. All the scale bars are 100 μ m.

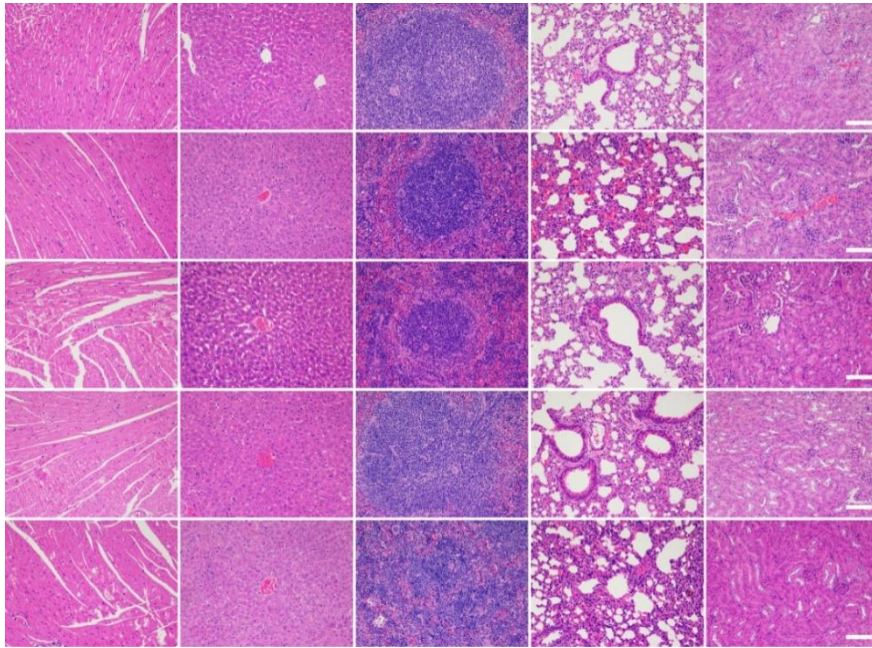


Figure S10. H&E staining of major organs from the experimental group 3 days post intravenous injection of Lip-Mel. All the scale bars are 100 μm .

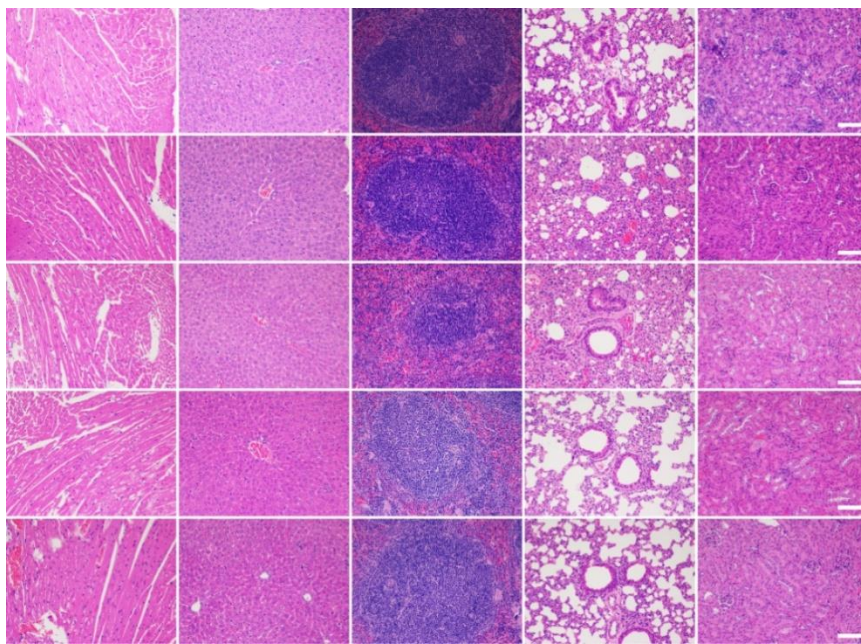


Figure S11. H&E staining of major organs from the experimental group 3 days post intravenous injection of Lip. All the scale bars are 100 μm .

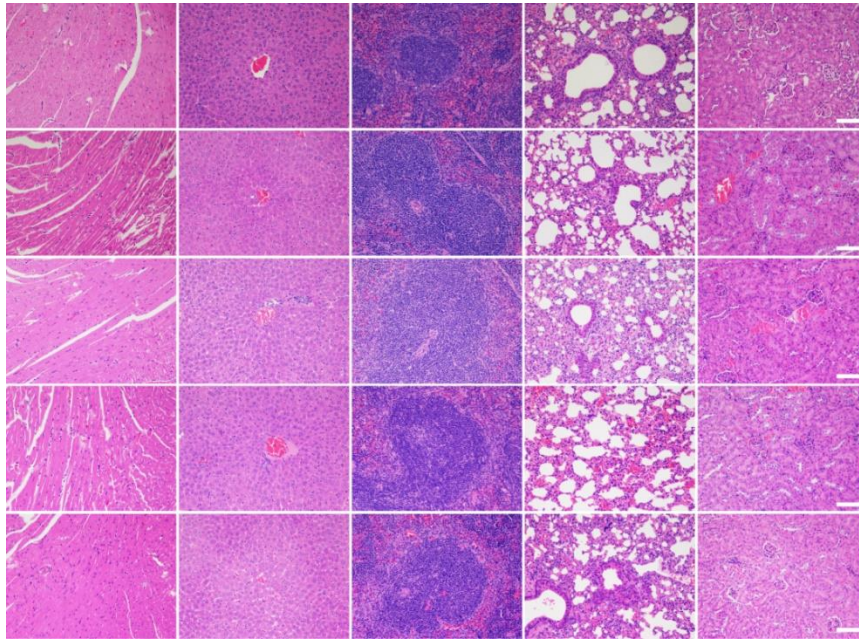


Figure S12. H&E staining of major organs from the experimental group 3 days post intravenous injection of Mel. All the scale bars are 100 μm .

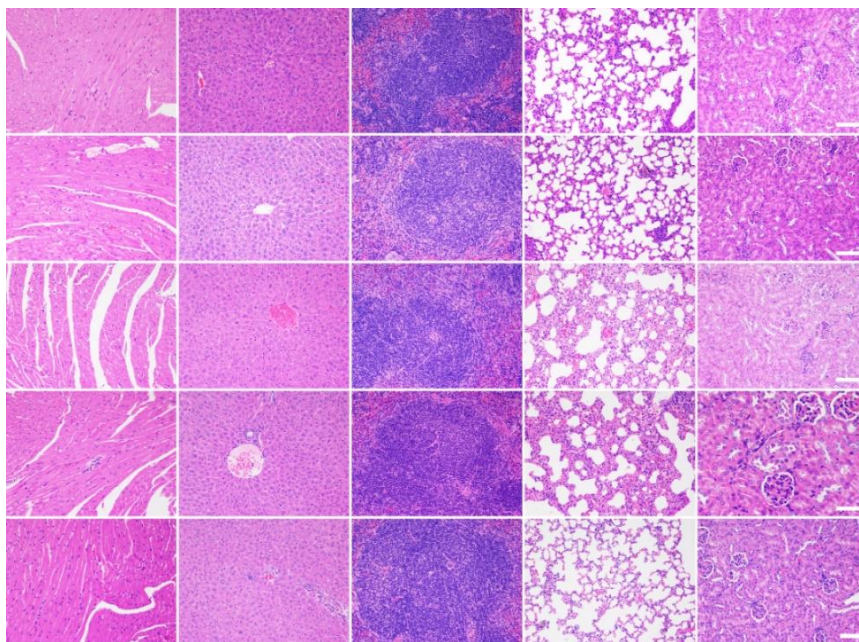


Figure S13. H&E staining of major organs from the experimental group 7 days post intravenous injection of Lip-Mel. All the scale bars are 100 μm .

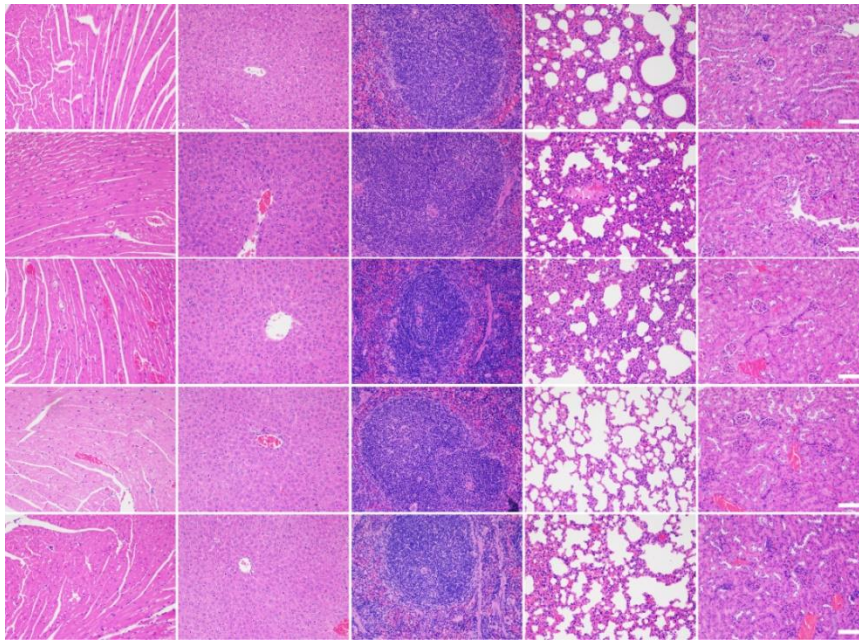


Figure S14. H&E staining of major organs from the experimental group 7 days post intravenous injection of Lip. All the scale bars are 100 μ m.

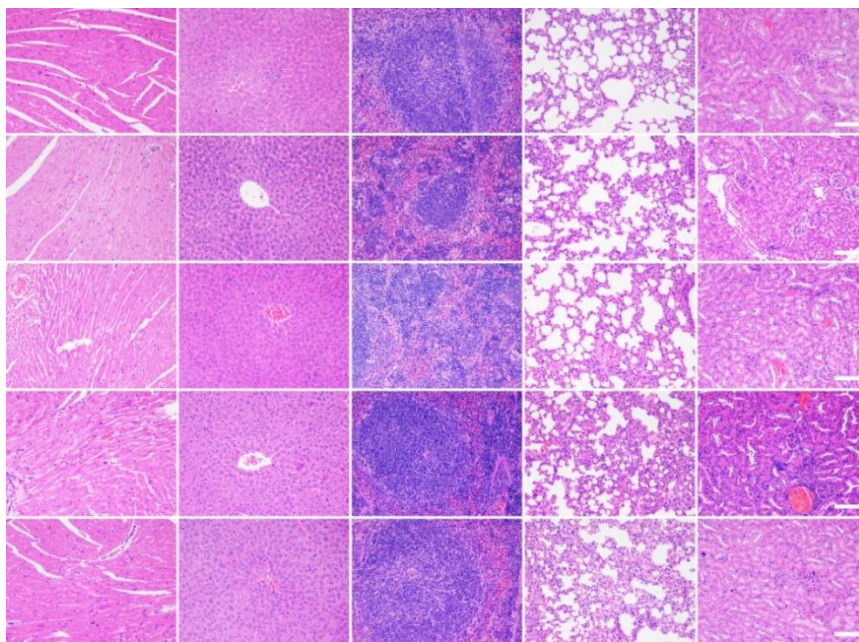


Figure S15. H&E staining of major organs from the experimental group 7 days post intravenous injection of Mel. All the scale bars are 100 μ m.

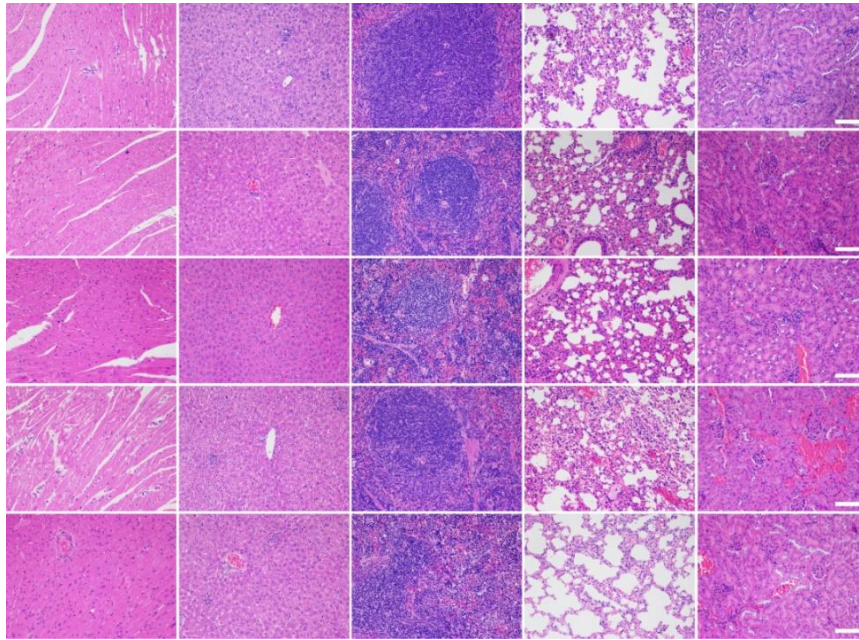


Figure S16. H&E staining of major organs from the experimental group 14 days post intravenous injection of Lip-Mel. All the scale bars are 100 μm .

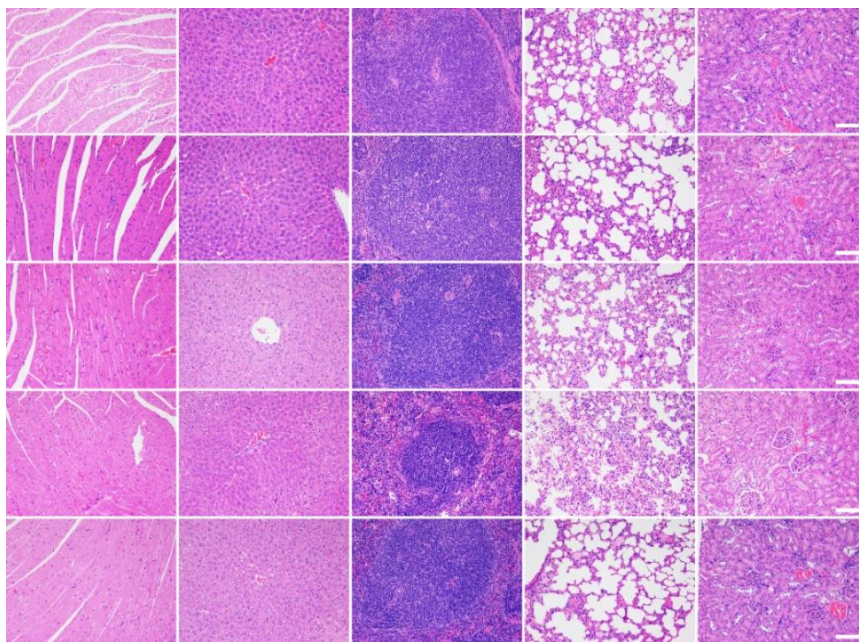


Figure S17. H&E staining of major organs from the experimental 14 days post intravenous injection of Lip. All the scale bars are 100 μm .

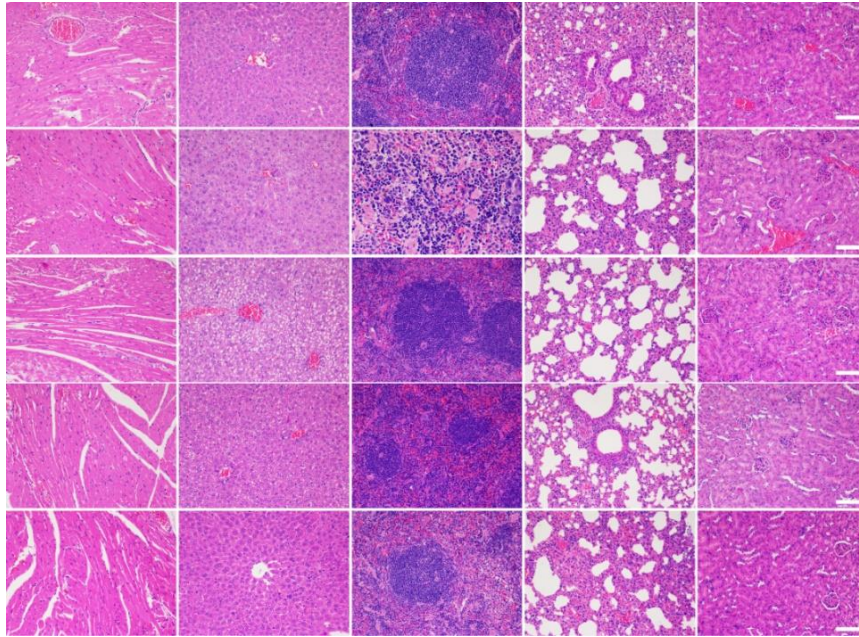


Figure S18. H&E staining of major organs from the experimental group 14 days post intravenous injection of Mel. All the scale bars are 100 μ m.

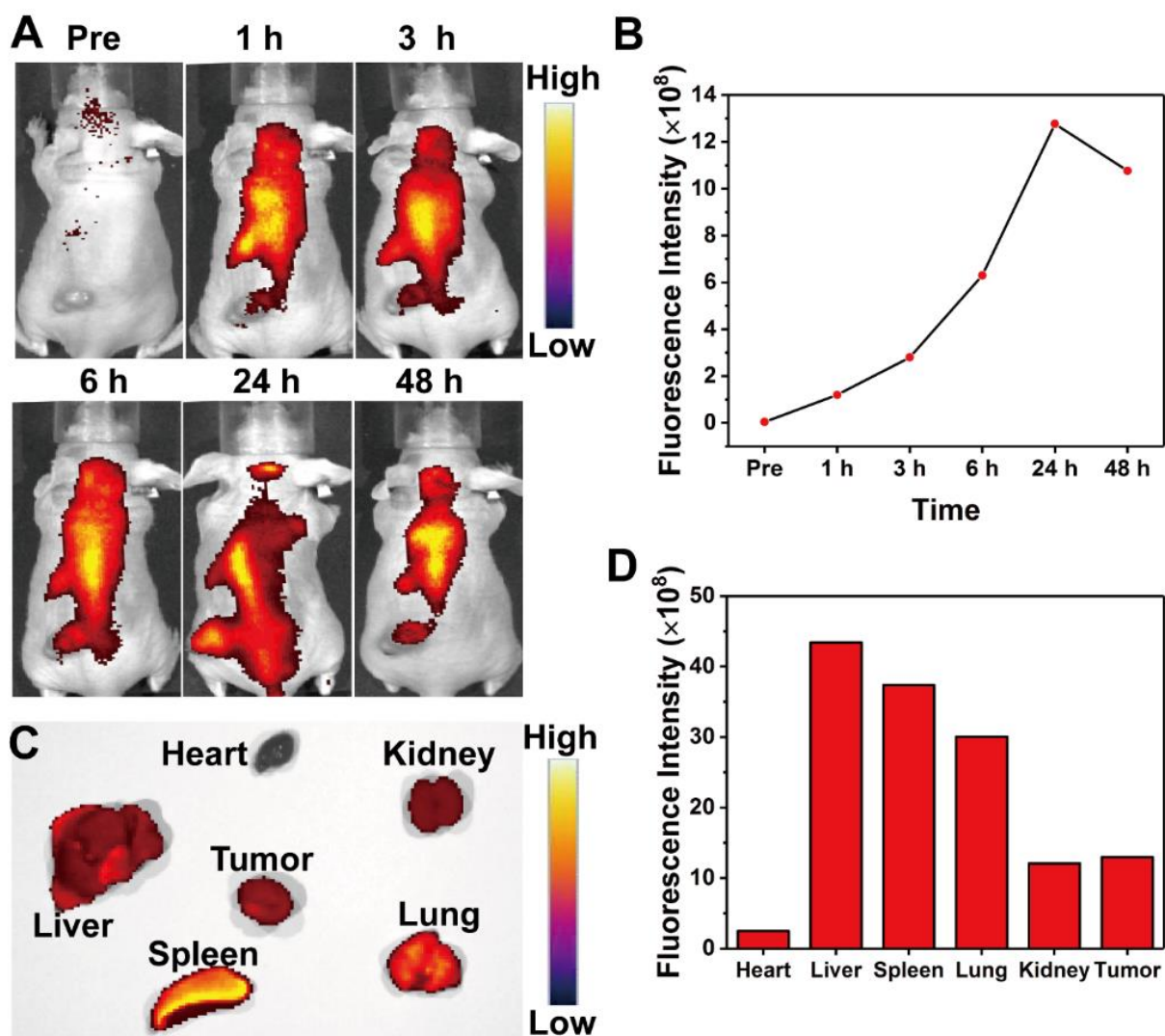


Figure S19. *In vivo* bio-distribution of Lip-Mel. **(A)** *In vivo* fluorescence images of tumor after intravenous injection of Lip-Mel labeled with DiR at different time points. **(B)** Quantitative tumor fluorescence signal intensities at corresponding time points. (n = 3, mean \pm SD). **(C)** *Ex vivo* fluorescence images of major organs and tumor dissected from mice at 24 h post injection. **(D)** Quantitative bio-distribution of Lip-Mel in mice.

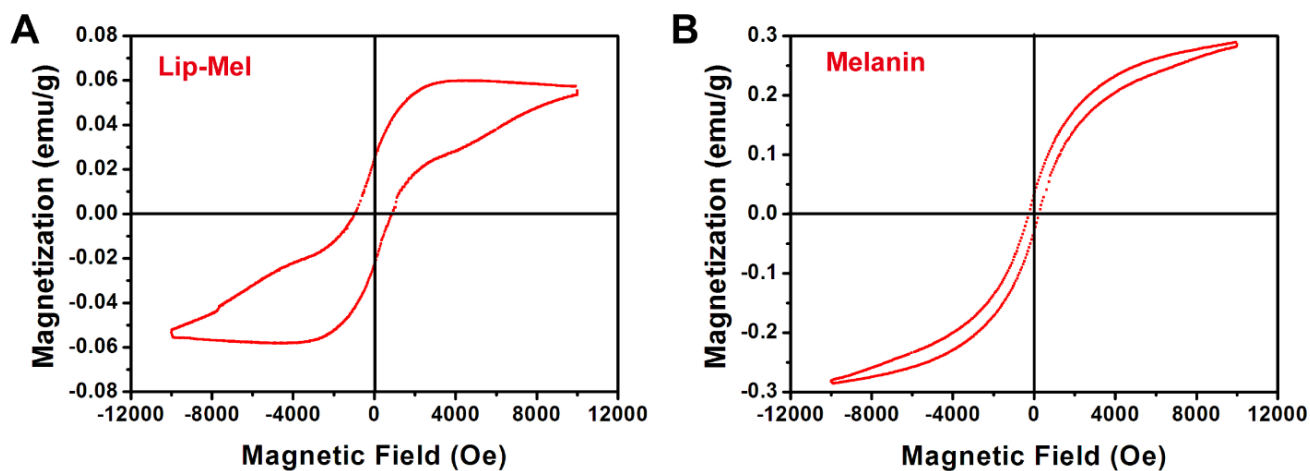


Figure S20. Magnetization hysteresis loops of (A) Lip-Mel and (B) melanin at 300 K in the range of $-12 \text{ kOe} < H < +12 \text{ kOe}$.

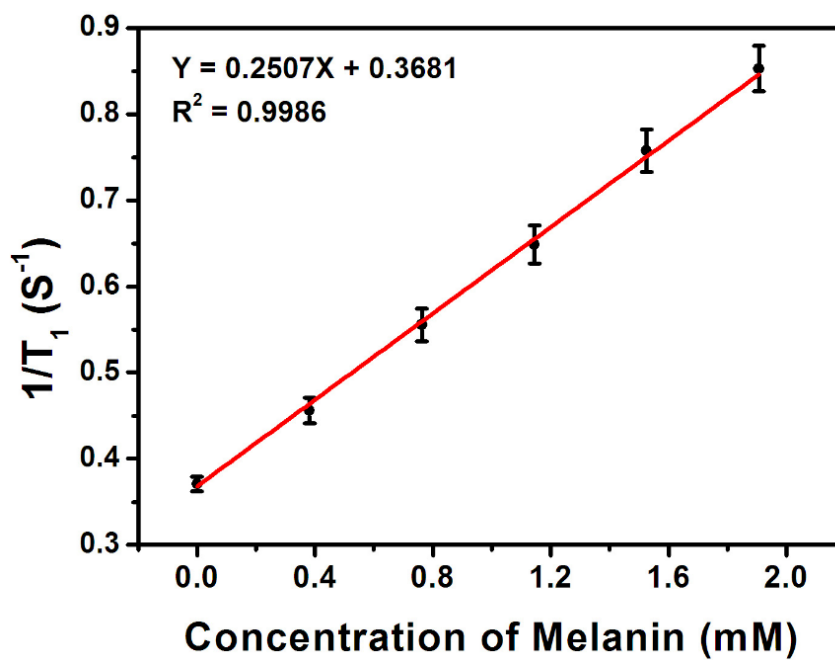


Figure S21. Plot of $1/T_1$ as a function of melanin concentration in Lip-Mel. The slope of the curve is defined as the specific relativity of r_1 .

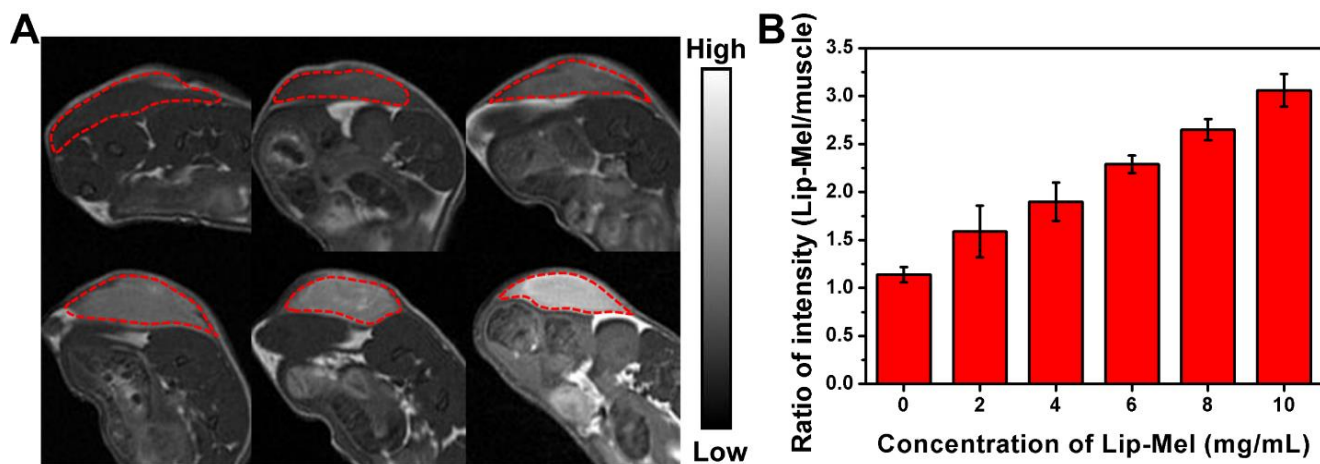


Figure S22. (A) T₁-weighted MRI detection of Lip-Mel in living mice. Mice were injected subcutaneously (region enveloped by red dotted line) with Lip-Mel at concentrations of 0, 2, 4 (from left to right in upper layer), and 6, 8, 10 (from left to right in bottom layer) mg/mL. (B) Ratio of intensity (Lip-Mel/muscle) at different concentrations of Lip-Mel.

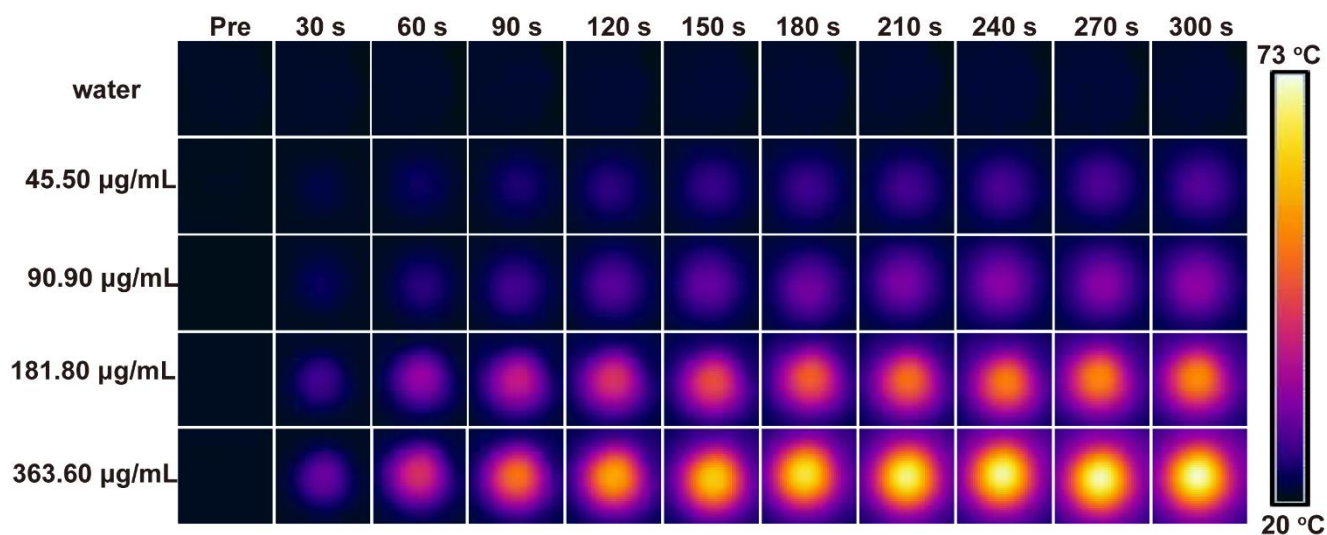


Figure S23. IR thermal images of pure water and Lip-Mel suspension at different concentrations (45.45, 90.90, 181.80, 363.60 µg/mL) as a function of irradiation duration using an 808 nm laser (1.50 W/cm²).

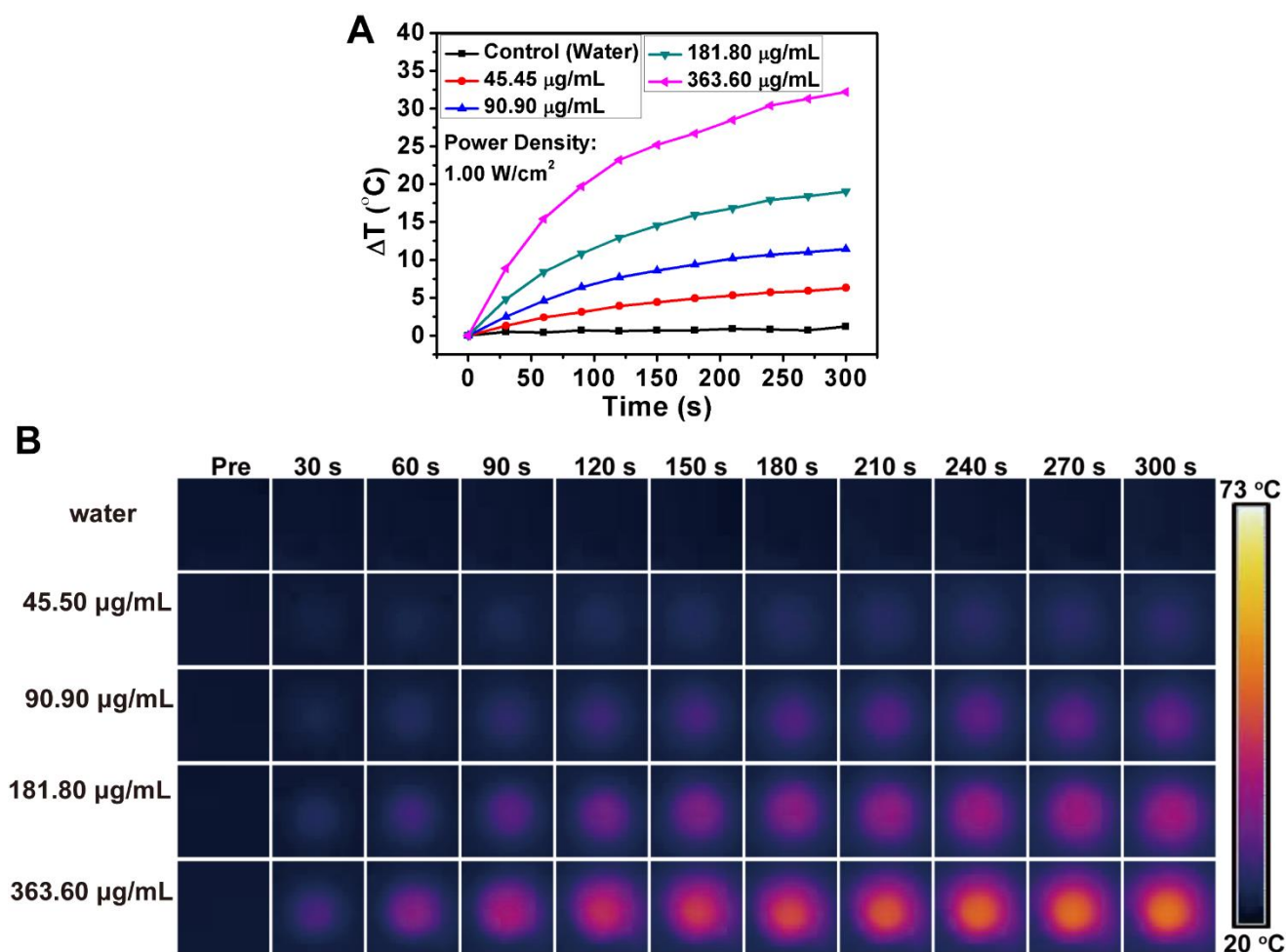


Figure S24. (A) Plot of temperature change (ΔT) and (B) IR thermal images of pure water and Lip-Mel suspension at different concentrations (45.45, 90.90, 181.80, 363.60 $\mu\text{g/mL}$) as a function of irradiation duration using an 808 nm laser (1.00 W/cm^2).

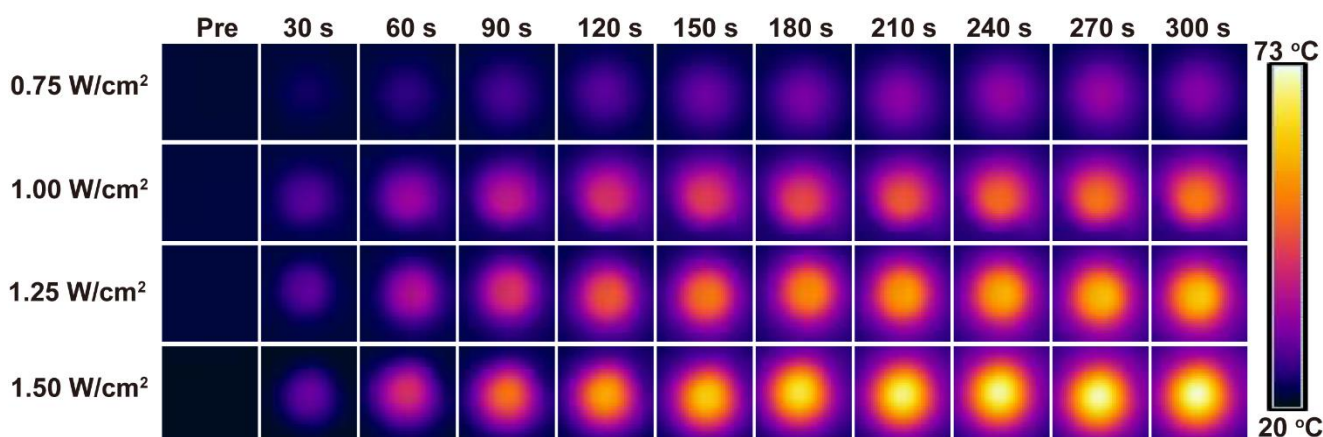


Figure S25. IR thermal images of Lip-Mel suspension at different power densities of an 808 nm laser (0.75, 1.00, 1.25 and 1.50 W/cm^2) as a function of irradiation duration (melanin concentration: 363.60 $\mu\text{g/mL}$, 100 μL).

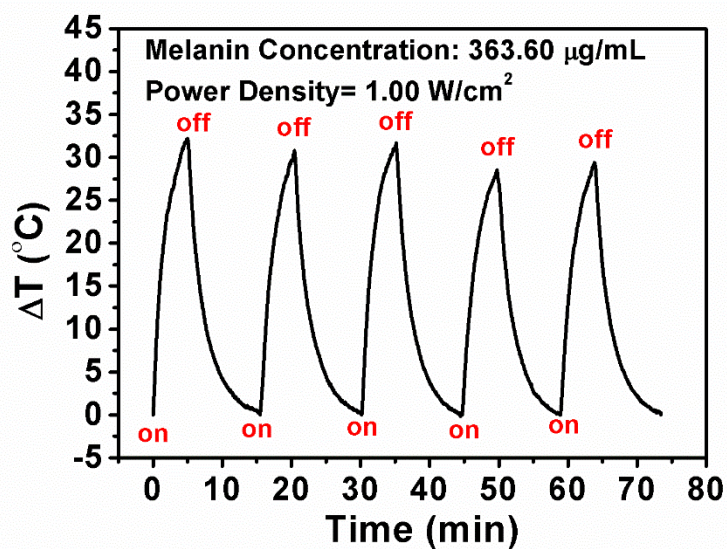


Figure S26. Recycling heating profiles of Lip-Mel (melanin concentration: 363.60 $\mu\text{g/mL}$, 100 μL) as irradiated by an 808 nm laser (1.00 W/cm^2) for five laser on/off cycles.

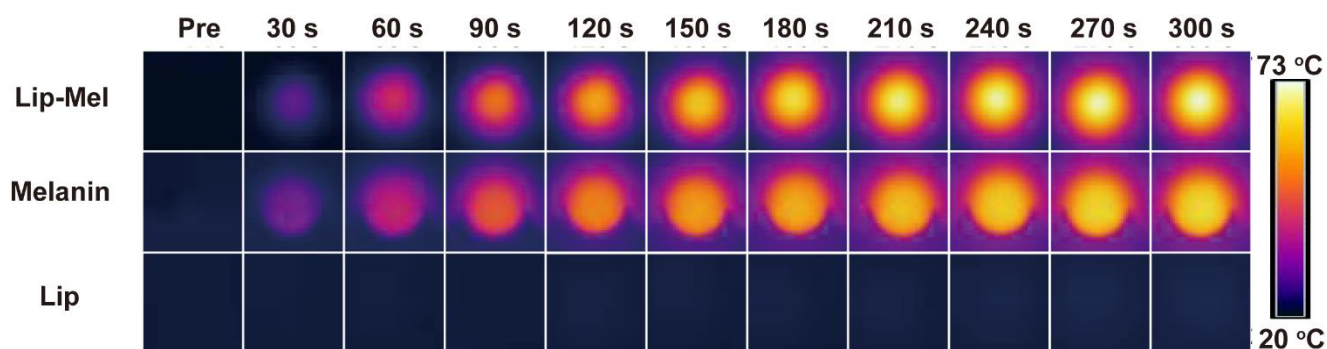


Figure S27. IR thermal images of Lip-Mel (melanin concentration: 363.60 $\mu\text{g/mL}$), melanin (363.60 $\mu\text{g/mL}$) and Lip suspension as a function of irradiation duration using an 808 nm laser (1.50 W/cm^2).

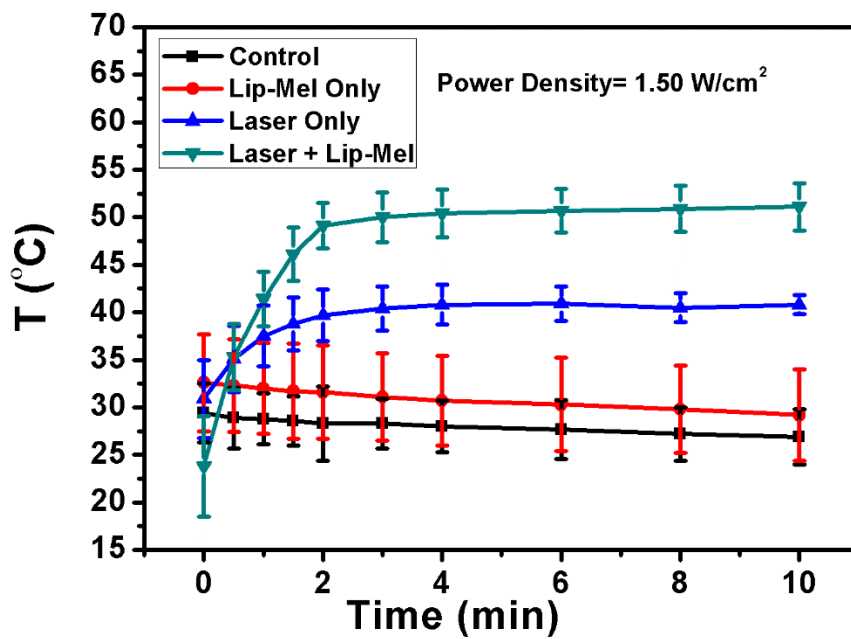


Figure S28. Temperature changes of MDA-MB-231 tumor regions of the four groups (control, Lip-Mel only, Laser only and Lip-Mel + Laser group) as a function of irradiation duration using an 808 nm laser (1.50 W/cm², 10 min).